

# Text2AC-Zero: Consistent Synthesis of Animated Characters using 2D Diffusion

Abdelrahman Eldesokey  
KAUST  
Thuwal, Saudi Arabia

abdelrahman.eldesokey@kaust.edu.sa

Peter Wonka  
KAUST  
Thuwal, Saudi Arabia

peter.wonka@kaust.edu.sa



Prompt: “A mechanical cyborg moves to the left on a sandy beach”



Prompt: “An astronaut jumps on the moon surface”



Prompt: “A man shimmy dances in a studio”

Figure 1. Text2AC-Zero produces temporally consistent videos of animated characters using pre-trained Text-to-Image diffusion.

## Abstract

We propose a zero-shot approach for consistent Text-to-Animated-Characters synthesis based on pre-trained Text-to-Image (T2I) diffusion models. Existing Text-to-Video (T2V) methods are expensive to train and require large-scale video datasets to produce diverse characters and motions. At the same time, their zero-shot alternatives fail to produce temporally consistent videos. We strive to bridge this gap, and we introduce a zero-shot approach that produces temporally consistent videos of animated characters

and requires no training or fine-tuning. We leverage existing text-based motion diffusion models to generate diverse motions that we utilize to guide a T2I model. To achieve temporal consistency, we introduce the Spatial Latent Alignment module that exploits cross-frame dense correspondences that we compute to align the latents of the video frames. Furthermore, we propose Pixel-Wise Guidance to steer the diffusion process in a direction that minimizes visual discrepancies. Our proposed approach generates temporally consistent videos with diverse motions and styles, outperforming existing zero-shot T2V approaches in

terms of pixel-wise consistency and user preference.

## 1. Introduction

Human synthesis is an essential task in computer vision and graphics, with several applications in movie production, art, and fashion. It aims to generate high-quality and diverse images/videos of human characters that adhere to some given conditions. For instance, in fashion, several approaches were proposed to perform novel view synthesis conditioned on a human pose [1, 21], virtual try-on given a new style [3], and video generation based on textual prompts [11]. Even though these approaches can produce high-quality and realistic output, they are domain-specific and are limited to specialized datasets [15]. More specifically, they can generate images/videos of fashion performers in controlled settings but not diverse characters in complex environments.

Text-to-Image (T2I) diffusion models [20, 22, 23] revolutionized the task of image synthesis by harnessing large-scale datasets with billions of image/text pairs [24]. Additional conditioning signals such as human pose and depth maps introduced in ControlNet [31] and T2I-Adapters [18] imposed further control over T2I models. This allowed the generation of highly diverse, faithful, and realistic images of human characters based on various conditioning signals. On the other hand, generating videos of human characters using Text-to-Video (T2V) diffusion models still lags behind due to the complexities associated with training these models. These complexities include modeling the temporal dimension, finding sufficiently large datasets, and fulfilling their excessive computational needs. As an example, the largest publicly available video dataset encompasses only 10 million videos [2], and it requires up to 48 A100-80GB GPUs to train the temporal module of VideoLDM [4].

Alternatively, several one and zero-shot approaches [5, 29, 29] leveraged T2I models to generate videos. Nevertheless, the output from these approaches lacks temporal consistency, and the generated contents tend to drift and flicker. To examine this behavior, we conduct a controlled experiment where we generate a short video using Text2Video-Zero [13] conditioned on depth maps. We obtain these depth maps by rendering a SMPL human model [16] and shifting it upwards by 10 pixels to simulate a moving human in a video, Figure 2 illustrates this experiment, and it shows that Text2Video-Zero fails to produce temporally consistent images even with this simple change to the conditioning signal. We find that this is caused by the distributional shift in the latent codes that are responsible for generating the character in the scene as shown on the right of Figure 2. This is similar to the findings of [4, 8], where they trained a temporal module on video datasets to align the latents of a T2I diffusion model. However, as mentioned earlier, training these temporal modules is computationally expensive and

requires large-scale video datasets.

In this paper, we propose a zero-shot approach for aligning the latents of T2I diffusion models that allows generating consistent videos of animated characters. We employ text-based human motion diffusion models [6, 28] to generate a sequence of guidance signals given a text prompt. Then, we use a pre-trained T2I model to generate the video frames conditioned on these guidance signals. To achieve temporal consistency between frames, we introduce the *Spatial Latent Alignment* module that attempts to align the latent codes between video frames based on a pre-computed cross-frame dense correspondence. Finally, we propose a *Pixel-Wise Guidance* strategy that steers the diffusion process in a direction that minimizes the visual discrepancies between frames. To evaluate temporal consistency, we introduce the *Human Mean Squared Error* metric that measures the pixel-wise difference of the animated character between consecutive frames. Our proposed approach outperforms existing zero-shot T2V approaches on this metric by  $\sim 10\%$  and was preferred by 76% of the users in a user study that we conducted.

Our contributions can be summarized as follows:

- We introduce a zero-shot video synthesis approach for animated characters that leverages pre-trained motion and T2I diffusion models.
- We propose the *Spatial Latent Alignment* and *Pixel-Wise Guidance* modules that boost temporal consistency between frames based on cross-frame dense correspondences that we compute.
- Our approach outperforms existing zero-shot approaches in terms of the *Human Mean Squared Error* metric that we introduce and in terms of user preference.

## 2. Related Work

We give a brief overview of existing approaches for human video synthesis, Text-to-Video (T2V) diffusion models, and human motion synthesis.

**Human Video Synthesis** Existing approaches for human video generation are generally limited to specific domains and datasets. For instance, several T2V approaches [17, 25, 30] train on the UCF-101 dataset [27] that includes videos of humans performing 101 diverse actions. However, the generated videos based on this dataset are low resolution and lack visual diversity. Another category of approaches focused on generating videos of fashion performers and is trained on fashion datasets [11, 15]. For instance, Text2Performer [11] proposed a decomposed human representation into pose and appearance in the latent space of a variational autoencoder. This representation is used alongside a diffusion-based motion sampler to generate consistent high-resolution videos of fashion performers. Nevertheless, their approach can only generate videos of performers with standardized motions on a simple background. Our

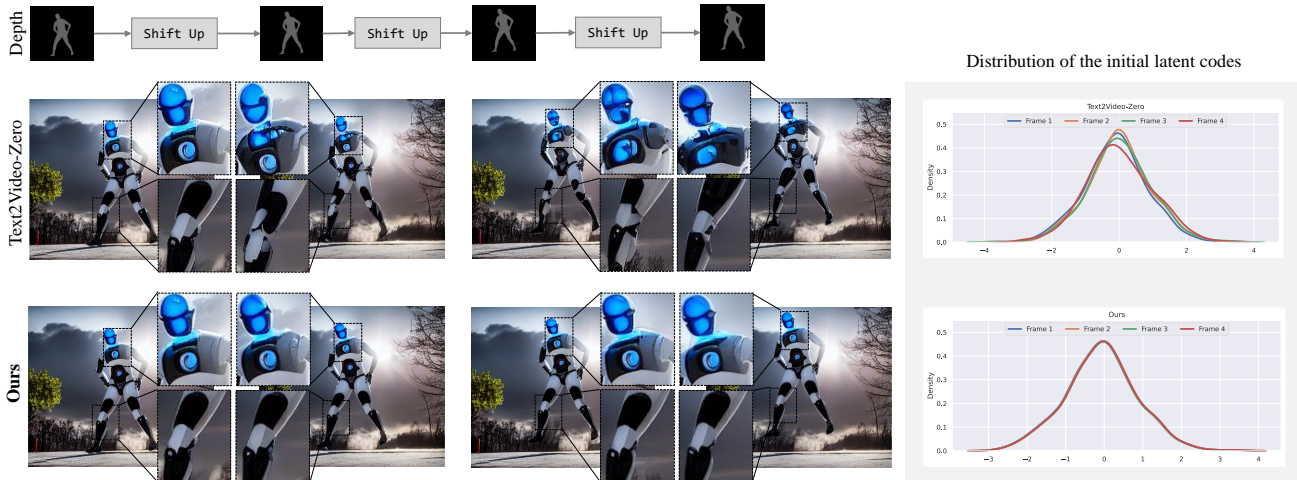


Figure 2. Latent diffusion models for Text-to-Image (T2I) synthesis are sensitive to changes in the latent codes. For instance, if we condition Text2Video-Zero [13] on a depth map and then shift this map upwards by 10 pixels, the textures on the generated character (the robot) change dramatically. By examining the distributions of the initial latent codes that are aligned with the character, we observe a distributional shift, as shown on the plot to the right. Our proposed approach attempts to align the latent codes in a zero-shot manner, eliminating the distribution shift and producing consistent images, as shown at the bottom right.

approach aims to generate videos of any human-like characters (*e.g.* fictional characters) performing diverse actions in complex environments.

**Text-to-Video Diffusion Models** Text-to-Image (T2I) diffusion models [20, 22, 23] excelled in generating highly realistic and diverse images based on textual prompts by harnessing large-scale image datasets [24]. With the lack of similarly large video datasets to train T2V counterparts, a growing direction of research attempts to exploit existing T2I models to generate videos. VideoLDM [4] proposed to transform a pre-trained Stable Diffusion model [22] into a T2V model by introducing a temporal module and a video upsampler that are trained on video data. Similarly, Make-a-video [25] extended DALLE-2 [20] to a T2V model by temporally aligning the decoder and the upsampler on video data. However, these two approaches require excessive GPU resources to train and are limited by the scale of the available video datasets.

Tune-a-Video [29] adopts a one-shot paradigm and fine-tunes a pre-trained T2I model to generate a video given a single video/text pair. Nevertheless, this approach requires a video as an input in addition to the text prompt making it more suitable for video editing or Video-to-Video tasks. Text2Video-Zero [13] introduced a purely text-based zero-shot T2V approach that injects motion dynamics into the latents of a T2I diffusion model. Their approach exploited the fact that the output of diffusion models varies under any changes to the latent codes to generate variations of the first frame. However, the generated frames from their approach lack any motion continuity or temporal consistency. In con-

trast, our approach produces temporally consistent videos of human characters with continuous motion.

**Human Motion Synthesis** This task aims to produce animated skeletons (standardized poses) of humans conditioned on textual prompts. Several approaches for human motion synthesis were proposed that benefited from the large datasets for human motions, such as the HumanML3D dataset [10] with approximately 15k diverse motions. T2M [10] proposed a two-stage approach that learns a mapping function between text prompt and motion length. Afterward, a temporal variational autoencoder generates the motion given the predicted length. MDM [28] employed a diffusion model to learn a conditional mapping between text and motion sequences. MLD [6] learns a compact latent representation to train diffusion models in a more efficient manner. GMD [12] incorporated spatial constraints into the motion diffusion process to add more control over the generated motions. We employ any of these approaches to generate diverse and continuous motion signals to guide a pre-trained T2I diffusion model.

### 3. Method

In this section, we first describe the existing pipeline for zero-shot Text-to-Video (T2V) diffusion models that is adopted by Text2Video-Zero [13] and MasaCtrl [5]. Then, we explain our proposed zero-shot approach for generating temporally consistent and continuous videos of animated characters.

### Zero-Shot Text-to-Animated-Characters

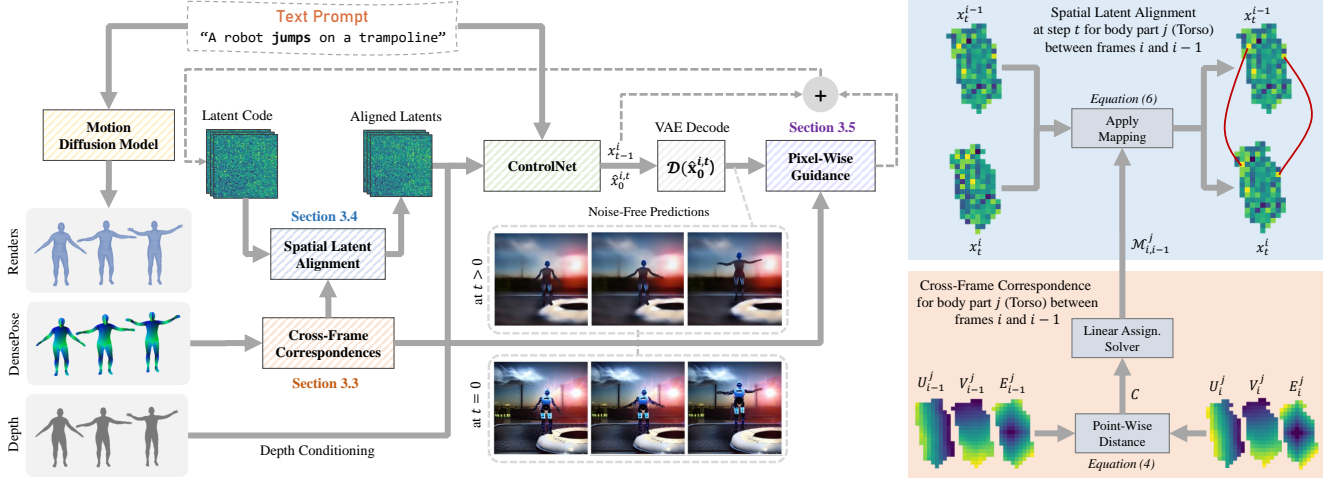


Figure 3. An overview of our proposed approach. Given a text prompt  $\mathcal{T}$ , a motion diffusion model [28] produces a sequence of human skeletons that we use to obtain frame-wise depth maps and DensePose [9]. The former is used as guidance for ControlNet [31], while the latter is used to compute cross-frame correspondences. These correspondences are employed by the Spatial Latent Alignment and the Pixel-Wise Guidance modules to boost temporal consistency. The orange block shows an illustration of how we compute cross-frame correspondences between two frames for the “torso” body part based on DensePose. The blue block shows how we employ these correspondences to spatially align the latents to promote consistent synthesis.

### 3.1. Zero-Shot T2V Diffusion Models

The objective of the T2V task is to generate a sequence of  $N$  video frames  $\mathcal{I} := \{I_1, I_2, \dots, I_N\}$ , given a text prompt  $\mathcal{T}$ . In the zero-shot setting, a pre-trained Text-to-Image (T2I) diffusion model such as Stable Diffusion (SD) [22] is used to generate each frame individually. For better control over the contents of the generated frames, additional conditioning signals  $\mathcal{G} := \{G_1, G_2, \dots, G_N\}$ , such as human poses, canny edges, and depth maps are incorporated through ControlNet [31] or T2I-Adapters [18].

During inference, the diffusion process is carried out using a denoising model such as DDIM [26], where for each frame  $i$  and denoising step  $t$ , we compute the previous latent code  $x_{t-1}^i$  as well as, a noise-free sample prediction  $\hat{x}_0^{i,t}$ :

$$\hat{x}_0^{i,t} = \frac{x_t^i - \sqrt{1 - \alpha_t} \epsilon_\theta^t(x_t^i, \mathcal{T}, G_i)}{\sqrt{\alpha_t}}, \quad (1)$$

$$x_{t-1}^i = \sqrt{\alpha_{t-1}} \hat{x}_0^{i,t} + \sqrt{1 - \alpha_{t-1} - \sigma_t^2} \epsilon_\theta^t(x_t^i, \mathcal{T}, G_i) + \sigma_t \epsilon_t, \quad (2)$$

where  $\alpha_t, \sigma_t$  are pre-defined scheduling parameters,  $\epsilon_\theta^t$  is a noise prediction from a trained UNet, and  $\epsilon_t$  is random Gaussian noise. This process is computed for  $T \geq t \geq 0$ , and the final image is reconstructed at  $t = 0$  using the decoder of a variational autoencoder as  $I_i = \mathcal{D}(\hat{x}_0^{i,0})$ . To promote visual consistency, the initial latent code  $x_T$  is shared among all frames, and the self-attention modules are replaced with cross-frame attention. We refer the reader to

[5, 13] for details on cross-frame attention. We use this aforementioned pipeline as a baseline for our approach.

### 3.2. Zero-Shot Text-to-Animated-Characters

To generate videos of animated characters using T2I models, we need conditioning signals  $\mathcal{G}$  to control the generated content. Existing methods [13, 29] extract these signals from a user-provided video. For example, a depth or human pose detector is applied to a video to extract depth maps or human poses. However, this approach has limited control over the generated content and adds the burden of finding a suitable video.

Instead, we propose to employ text-based motion diffusion models [6, 28] to produce a sequence of length  $N$  of human skeletons, given the text prompt  $\mathcal{T}$ . Afterward, we fit a customizable human body model such as SMPL [16] to each of these skeletons, and we render  $N$  depth maps from these models to produce conditioning signals  $\mathcal{G}^{depth}$ . We also compute DensePose [9] for each frame to obtain  $\mathcal{P} := \{P_1, P_2, \dots, P_N\}$ . This approach eliminates the need for providing a reference video as in [5, 13, 29] and makes the process purely text-driven. An overview of our proposed approach is illustrated in Figure 3.

### 3.3. Cross-Frame Dense Correspondences

Since we obtained per-frame conditioning signals  $\mathcal{G}^{depth}$ , we can directly generate the video frames. However, as demonstrated in Figure 2, the output of SD varies under any changes to the conditioning signal, causing the frames to be

temporally inconsistent. To alleviate this problem, the latent codes during inference must be spatially aligned, *i.e.*, each body part of the generated character needs to have the same latent code in all frames. To achieve this, we need to compute pixel-wise dense correspondences between frames and use them to propagate the latent codes across frames.

DensePose provides pixel-wise embeddings for the human body. Nonetheless, the DensePose detector is not temporally-aware, meaning that a given body point is not guaranteed to have the same embedding in all frames. Moreover, downsampling the DensePose embeddings to the latent resolution encompasses quantization, which will misalign the embeddings further. To tackle this issue, we set up a dense correspondence problem between each two consecutive frames based on the DensePose embeddings. The embedding for frame  $i$  is denoted as  $P_i = [L_i, U_i, V_i]$ , where  $P_i \in \mathcal{P}$ ,  $L_i$  has pixel-wise labels for body parts in the range of  $[0, 24]$ , and  $U_i, V_i$  are UV-coordinates in the range of  $[0, 255]$ . For each body part  $j$ , we define a set of pixels that belong to that part as  $Q_i^j := \{q \mid L_i(q) = j\}$ . We form a feature vector for each  $q \in Q_i^j$  and we arrange them in the rows of matrix  $\hat{P}_i^j$ :

$$\hat{P}_i^j[q] = [U_i^j(q) \quad V_i^j(q) \quad E_i^j(q)] \quad , \quad (3)$$

where  $E_i^j[q]$  is the euclidean distance between pixel  $q$  and the centroid of body part  $j$ . This term encourages the matching of pixels that are spatially close.

For each two consecutive frames  $i$  and  $i-1$ , we compute a cost matrix  $C$  between  $\hat{P}_i^j$  and  $\hat{P}_{i-1}^j$  as:

$$C[q, s] = \|\hat{P}_i^j[q] - \hat{P}_{i-1}^j[s]\|_2 \quad , \quad (4)$$

where  $q \in Q_i^j, s \in S_{i-1}^j$ , and  $S_{i-1}^j := \{s \mid L_{i-1}(s) = j\}$ . Then, we find the correspondences by solving a linear assignment problem over  $C$  using the Hungarian algorithm [14], which assigns each pixel to the closest match based on the UV coordinates and the spatial location. This produces an *injective* mapping for each body part  $j$  between frames  $i$  and  $i-1$  as:

$$\mathcal{M}_{i,i-1}^j := \{(q, s) \mid q \in Q_i^j, s \in S_{i-1}^j\} \quad , \quad (5)$$

An illustration for this procedure is shown in Figure 3. Finally, All body parts are then combined into a total body mapping as  $\mathcal{M}_{i,i-1} = \cup_j \mathcal{M}_{i,i-1}^j$ .

### 3.4. Spatial Latent Alignment

To achieve temporal consistency, we aim to align the latents between the video frames. We compute correspondence mappings from Section 3.3 between each two consecutive frames based on DensePose embeddings  $\mathcal{P}$  that are downsampled to  $64 \times 64$  to match the resolution of the latent

---

### Algorithm 1 Zero-Shot Animated Characters Synthesis

---

**Require:**  $N, T \in \mathbb{N}, \delta \in \mathbb{R}$ , text prompt  $\mathcal{T}$ ,  $A := [a_1, a_2]$ ,  $B := [b_1, b_2]$  ControlNet (CN), DDIM (DDIM), Motion Diffusion Model (MDM), Spatial Latent Alignment (ALIGN), Pixel-Wise Refinement (REFINE)

**Output:**  $\mathcal{I} := \{I_1, I_2, \dots, I_N\}$   
 $\mathcal{G}^{depth}, \mathcal{P} \leftarrow \text{MDM}(\mathcal{T})$  ▷ Depth maps, DensePose  
 $x_T \sim \mathcal{N}(0, I)$   
**for**  $i = 1, \dots, N$  **do**  
  **for**  $t = T, T-1, \dots, 0$  **do**  
    **if**  $i > 1$  and  $t \in A$  **then** ▷ Spatial Latent Alignment  
       $x_t^i \leftarrow \text{ALIGN}(x_t^i, \mathcal{P}[i], \mathcal{P}[i-1])$   
    **end if**  
     $\epsilon_\theta^t \leftarrow \text{CN}(x_t^i, \mathcal{T}, \mathcal{G}^{depth}[i], t)$   
     $x_{t-1}^i, \hat{x}_0^{i,t} \leftarrow \text{DDIM}(x_t^i, \epsilon_\theta^t)$   
    **if**  $i > 1$  and  $t \in B$  **then** ▷ Pixel-Wise Guidance  
       $\omega_i \leftarrow \text{REFINE}(\hat{x}_0^{i,t}, \mathcal{P}[i], \mathcal{P}[i-1])$   
       $x_{t-1}^i \leftarrow x_{t-1}^i - \delta \nabla_{x_t^i} \omega_i$   
    **end if**  
  **end for**  
**end for**

---

codes. For frames  $i$  and  $i-1$ , the latent code  $x_t^i$  is updated with values from  $x_t^{i-1}$  based on the computed mapping as:

$$x_t^i[q] = x_t^{i-1}[s] \quad \forall (q, s) \in \mathcal{M}_{i,i-1} \quad , \quad (6)$$

This operation will copy some parts of the latent code from frame  $i-1$  to the correct spatial location in frame  $i$ , promoting temporal consistency. Note that we only apply this operation at the first 40% of the diffusion steps that encompass the generation of the main structures of the scene.

### 3.5. Pixel-Wise Guidance

The resolution of the latents in SD is  $1/8$  of that of the generated images. Consequently, even after spatially aligning the latents in the Section 3.4, some high-resolution details will vary between the video frames. To alleviate this problem, we propose a Pixel-Wise Guidance strategy inspired by classifier guidance in diffusion models [19]. First, we compute a mapping  $\mathcal{M}_{i,i-1}$  from Section 3.3 between each two consecutive frames  $i$  and  $i-1$ . At a given diffusion step  $t$ , we reconstruct the RGB predictions using the VAE decoder as  $X_t^i = \mathcal{D}(\hat{x}_0^{i,t})$  and we compute the L2 difference between all pixel pairs in  $\mathcal{M}_{i,i-1}$ :

$$\omega_i = \sum_{q,s} (X_t^i[q] - X_t^{i-1}[s])^2 \quad \forall (q, s) \in \mathcal{M}_{i,i-1} \quad , \quad (7)$$

Finally, we compute the gradient of  $\omega_i$  with respect to  $x_t^i$ , and we use it to update  $x_{t-1}^i$ :

$$x_{t-1}^i = x_{t-1}^i - \delta \nabla_{x_t^i} \omega_i \quad . \quad (8)$$

where  $\delta$  is a scaling factor. This steers the diffusion process in the direction that minimizes  $\omega_i$ .

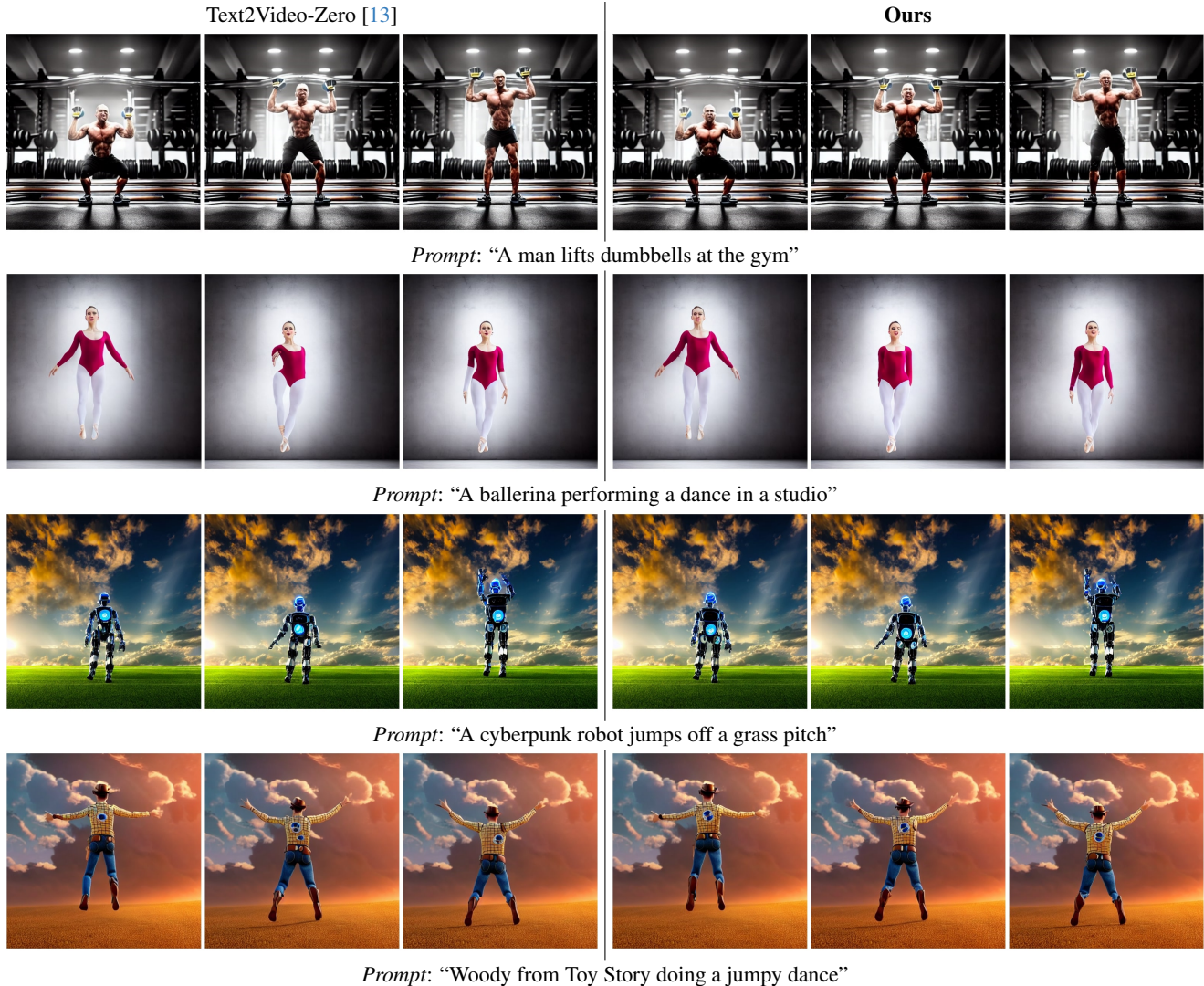


Figure 4. A qualitative comparison between our proposed approach and the baseline Text2Video-Zero [13]. Our approach is able to generate consistent shapes and textures compared to the baseline.

Note that we apply this process on the resolution of  $256 \times 256$  rather than the full resolution of  $512 \times 512$  as the latter would be computationally expensive. This is caused by the cubic complexity of the Hungarian algorithm that is used in Section 3.3.

## 4. Experiments

We evaluate our approach based on two baselines by incorporating our approach into their pipelines. The first baseline is MasaCtrl [5], which is an image editing method that can be used to generate a sequence of consistent images, and the second is Text2Video-Zero [13], a zero-shot approach for video synthesis. We also include some qualitative results for a trained T2V approach, Gen-2 [7].

### 4.1. Implementation Details

For both baselines, we use a pre-trained Stable Diffusion [22] version 1.5 with ControlNet [31] depth control to generate  $512 \times 512$  video frames. For inference, we employ the DDIM sampler [26] with a linear schedule. We use  $T = 100$  inference steps for Text2Video-Zero and  $T = 50$  for MasaCtrl. We empirically choose the guidance factor  $\delta = 0.01$  in Equation (8),  $A = [0, 39]$ ,  $B = [20, 69]$  for Text2Video-Zero, and  $A = [0, 19]$ ,  $B = [20, 39]$  for MasaCtrl in Algorithm 1. For motion synthesis, we use the official implementation of *Motion Diffusion Model (MDM)* [28] with some modifications for rendering and computing DensePose [9]. We conduct all experiments on a single NVIDIA A100 GPU except for Gen-2 [7], where we use



Figure 5. Impact of motion guidance in our approach compared to the motion dynamics in Text2Video-Zero [13]. Motion guidance produces videos that adhere to the prompt in contrast to Text2Video-Zero, which produces random variations of the scene.

the official online demo. Our code will be made publicly available on the project page <sup>1</sup>.

## 4.2. Qualitative Results

**Zero-Shot Comparison** Figure 4 shows a qualitative comparison between depth-conditioned Text2Video-Zero and our proposed approach. The first row shows that for Text2Video-Zero, the pants of the man in the first frame gradually change into shorts in the following frames, and the shape of the muscles changes between frames. On the other hand, our approach produces consistent clothing and muscles. In the second row, the body of the ballerina is distorted in the second frame of Text2Video-Zero, and the sleeves change color in the third frame. Our approach fixes the distorted frame and maintains the color of the sleeves. The third row shows that the circular light on the robot’s body changes location between frames in Text2Video-Zero. In contrast, our approach generated consistent textures. Finally, the last row shows the cowboy produced by Text2Video-Zero has an inconsistent texture on the shirt, the boots, and the belt. Our approach produces temporally consistent textures in all these regions. We provide more qualitative examples and comparisons against the other baseline MasaCtrl in the supplementary materials.

**Motion Guidance Significance** To demonstrate the impact of motion guidance produced by MDM, we compare our approach against Text2Video-Zero with no depth conditioning, which produces video by injecting motion dynamics into the latent codes. Figure 5 shows that Text2Video-Zero produces random variations of the scene that do not adhere to the motion in the prompt. For example, the astronaut in the top row is just floating and not jumping, and Ironman

<sup>1</sup><https://abdo-eldeskey.github.io/text2ac-zero/>

	$H_{MSE} \downarrow$	User Preference [%]
MasaCtrl [5] [ICCV23]	88.19	34 %
<b>Ours</b>	<b>79.88</b> (-9.4 %)	<b>66 %</b>
Text2Video-Zero [13] [ICCV23]	84.87	24 %
<b>Ours</b>	<b>76.41</b> (-10.0 %)	<b>76 %</b>

Table 1. Quantitative comparison between our proposed approach and two baselines. The error reduction percentage is shown

in the second row does not move but changes pose. On the other hand, our approach produces consistent videos that adhere to the motion in the prompt. We believe that our approach imposes more control over the generated videos as the animated skeletons from MDM can be used as a reference for many customizable human body models with different shapes, genders, and characteristics.

**Trained T2V Comparison** We also provide a comparison against the trained T2V model, Gen-2 [7], in Figure 6. In the first column, Gen-2 fails to produce a video of a robot jumping on a trampoline, and the robot morphs into a sphere. Our approach manages to produce a video for this uncommon scenario as the generation of the motion and the style are decoupled. In the second column, Gen-2 produces a good video of a skier with rich video dynamics. However, the skier loses his backpack after a few frames and deforms by the end of the video. Our approach produces a consistent video but with less background dynamics.

## 4.3. Quantitative Results

To numerically evaluate the generated videos, we introduce a new metric for temporal consistency and perform a user study. We denote the new metric as the *Human Mean Squared Error*  $H_{MSE}$ , and it compares the pixel-wise values of the generated characters in every two consecutive frames. We employ the computed cross-frame dense correspondences  $\mathcal{M}$  from Section 3.3, and we compute the mean squared error (MSE) between corresponding pixels:

$$H_{MSE} = \frac{1}{N} \sum_{i=1}^N \frac{1}{|\mathcal{M}_{i,i-1}|} \sum_{q,s} (I_i[q] - I_{i-1}[s])^2 \quad \forall (q,s) \in \mathcal{M}_{i,i-1} \quad (9)$$

where  $I_i, I_{i-1}$  are the final generated frames in  $\mathcal{I}$ .

We generated 10 videos of diverse motions and characters and we computed the proposed metric and performed the user study on them. The videos will be provided in the supplementary material. Table 1 shows that our approach outperforms both baselines in terms of  $H_{MSE}$  by  $\sim 9-10\%$  which demonstrates that the generated characters



Figure 6. A comparison against the trained T2V model Gen-2 [7].

	$H_{MSE} \downarrow$
Baseline (Text2Video-Zero [13])	84.87
with SLA	78.90 (-7.0 %)
with PWG	82.73 (-2.5 %)
with LSA + PWG	76.41 (-10.0 %)

Table 2. An ablation study for different components of our proposed approach. *SLA*: Spatial Latent Alignment in Section 3.4, *PWG*: Pixel-Wise Guidance in Section 3.5.

are temporally more consistent. For the user study, users are asked to select between two videos; one is produced by the baseline and the other by our approach. Table 1 shows that 76% and 66% of the users preferred the videos generated by our approach over Text2Video-Zero and MasaCtrl baselines, respectively.

#### 4.4. Ablation Study

We provide an ablation study in Table 2 to show the contribution of each component in our proposed pipeline to the overall performance. The Spatial Latent Alignment module contributes the most to the overall improvement and improves by 7.0% over the baseline. This indicates that aligning the latents plays a crucial role in achieving temporal consistency. Pixel-Wise Guidance in Section 3.5 improves over the baseline by 2.6% as it is mainly focused on the fine details. The two components combined achieve a joint improvement of 10 % compared to the baseline.

#### 4.5. Limitations and Failure Cases

Since we employ ControlNet with depth conditioning for generating the video frames, our approach is also bounded by its limitations. For example, the top row of Figure 7 shows an example where ControlNet fails to produce a realistic left arm and leg when they intersect in the depth map. Another source of failure is mismatches when computing the correspondence mapping in Section 3.3. These mis-

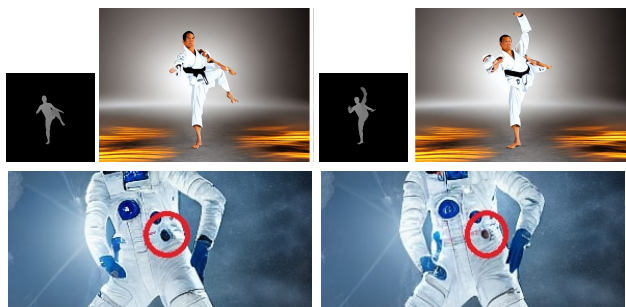


Figure 7. Examples of failure cases.

matches can lead to inconsistent texture, as shown in the second row of Figure 7. Despite that the Pixel-Wise Guidance module in Section 3.5 attempts to fix these discrepancies, sometimes it does not fully fix them due to insufficient scaling factor in Equation (8). It is also worth mentioning that Pixel-Wise Guidance imposes high GPU memory usage due to computing gradients with respect to the latent codes. However, employing the Spatial Latent Alignment solely still achieves remarkable improvement over the baseline as shown in Table 2 with no GPU memory overhead.

## 5. Conclusion and Future Work

We introduced a new paradigm for generating consistent videos of animated characters in a zero-shot manner. We employed text-based motion diffusion models to provide continuous motion guidance that we utilized to generate video frames through a pre-trained T2I diffusion model. This allowed generating videos of diverse characters and motions that existing T2V methods struggled to produce. We also demonstrated that our approach produces temporally consistent videos achieved through the proposed Spatial Latent Alignment and Pixel-Wise Guidance modules. We believe that these modules can benefit other latent diffusion-based approaches. For future work, the cross-

frame dense correspondences can be improved for better latent alignment. Furthermore, video dynamics can be incorporated into the background for enhanced realism.

## References

- [1] Badour AlBahar, Jingwan Lu, Jimei Yang, Zhixin Shu, Eli Shechtman, and Jia-Bin Huang. Pose with Style: Detail-preserving pose-guided image synthesis with conditional stylegan. *ACM Transactions on Graphics*, 2021. [2](#)
- [2] Max Bain, Arsha Nagrani, Gül Varol, and Andrew Zisserman. Frozen in time: A joint video and image encoder for end-to-end retrieval. In *Proceedings of the IEEE/CVF International Conference on Computer Vision*, pages 1728–1738, 2021. [2](#)
- [3] Ankan Kumar Bhunia, Salman Khan, Hisham Cholakkal, Rao Muhammad Anwer, Jorma Laaksonen, Mubarak Shah, and Fahad Shahbaz Khan. Person image synthesis via denoising diffusion model. In *Proceedings of the IEEE/CVF Conference on Computer Vision and Pattern Recognition*, pages 5968–5976, 2023. [2](#)
- [4] Andreas Blattmann, Robin Rombach, Huan Ling, Tim Dockhorn, Seung Wook Kim, Sanja Fidler, and Karsten Kreis. Align your latents: High-resolution video synthesis with latent diffusion models. In *IEEE Conference on Computer Vision and Pattern Recognition (CVPR)*, 2023. [2](#), [3](#)
- [5] Mingdeng Cao, Xintao Wang, Zhongang Qi, Ying Shan, Xiao-hu Qie, and Yinqiang Zheng. Masactrl: Tuning-free mutual self-attention control for consistent image synthesis and editing. *arXiv preprint arXiv:2304.08465*, 2023. [2](#), [3](#), [4](#), [6](#), [7](#), [1](#)
- [6] Xin Chen, Biao Jiang, Wen Liu, Zilong Huang, Bin Fu, Tao Chen, and Gang Yu. Executing your commands via motion diffusion in latent space. In *Proceedings of the IEEE/CVF Conference on Computer Vision and Pattern Recognition*, pages 18000–18010, 2023. [2](#), [3](#), [4](#)
- [7] Patrick Esser, Johnathan Chiu, Parmida Atighehchian, Jonathan Granskog, and Anastasis Germanidis. Structure and content-guided video synthesis with diffusion models. In *Proceedings of the IEEE/CVF International Conference on Computer Vision*, pages 7346–7356, 2023. [6](#), [7](#), [8](#)
- [8] Songwei Ge, Seungjun Nah, Guilin Liu, Tyler Poon, Andrew Tao, Bryan Catanzaro, David Jacobs, Jia-Bin Huang, Ming-Yu Liu, and Yogesh Balaji. Preserve your own correlation: A noise prior for video diffusion models. In *Proceedings of the IEEE/CVF International Conference on Computer Vision*, pages 22930–22941, 2023. [2](#)
- [9] Riza Alp Güler, Natalia Neverova, and Iasonas Kokkinos. Densepose: Dense human pose estimation in the wild. In *Proceedings of the IEEE conference on computer vision and pattern recognition*, pages 7297–7306, 2018. [4](#), [6](#), [1](#)
- [10] Chuan Guo, Shihao Zou, Xinxin Zuo, Sen Wang, Wei Ji, Xingyu Li, and Li Cheng. Generating diverse and natural 3d human motions from text. In *Proceedings of the IEEE/CVF Conference on Computer Vision and Pattern Recognition (CVPR)*, pages 5152–5161, 2022. [3](#)
- [11] Yuming Jiang, Shuai Yang, Tong Liang Koh, Wayne Wu, Chen Change Loy, and Ziwei Liu. Text2performer: Text-driven human video generation. In *Proceedings of the IEEE/CVF International Conference on Computer Vision*, 2023. [2](#)
- [12] Korrawe Karunratanakul, Konpat Preechakul, Supasorn Suwajanakorn, and Siyu Tang. Gmd: Controllable human motion synthesis via guided diffusion models. *arXiv preprint arXiv:2305.12577*, 2023. [3](#)
- [13] Levon Khachatryan, Andranik Movsisyan, Vahram Tadevosyan, Roberto Henschel, Zhangyang Wang, Shant Navasardyan, and Humphrey Shi. Text2video-zero: Text-to-image diffusion models are zero-shot video generators. *arXiv preprint arXiv:2303.13439*, 2023. [2](#), [3](#), [4](#), [6](#), [7](#), [8](#), [1](#)
- [14] Harold W Kuhn. The hungarian method for the assignment problem. *Naval research logistics quarterly*, 2(1-2):83–97, 1955. [5](#)
- [15] Ziwei Liu, Ping Luo, Shi Qiu, Xiaogang Wang, and Xiaoou Tang. Deepfashion: Powering robust clothes recognition and retrieval with rich annotations. In *Proceedings of IEEE Conference on Computer Vision and Pattern Recognition (CVPR)*, 2016. [2](#)
- [16] Matthew Loper, Naureen Mahmood, Javier Romero, Gerard Pons-Moll, and Michael J Black. Smpl: A skinned multi-person linear model. In *Seminal Graphics Papers: Pushing the Boundaries, Volume 2*, pages 851–866, 2023. [2](#), [4](#)
- [17] Zhengxiong Luo, Dayou Chen, Yingya Zhang, Yan Huang, Liang Wang, Yujun Shen, Deli Zhao, Jingren Zhou, and Tieniu Tan. Videofusion: Decomposed diffusion models for high-quality video generation. In *Proceedings of the IEEE/CVF Conference on Computer Vision and Pattern Recognition*, pages 10209–10218, 2023. [2](#)
- [18] Chong Mou, Xintao Wang, Liangbin Xie, Yanze Wu, Jian Zhang, Zhongang Qi, Ying Shan, and Xiaohu Qie. T2i-adapter: Learning adapters to dig out more controllable ability for text-to-image diffusion models. *arXiv preprint arXiv:2302.08453*, 2023. [2](#), [4](#)
- [19] Alex Nichol, Prafulla Dhariwal, Aditya Ramesh, Pranav Shyam, Pamela Mishkin, Bob McGrew, Ilya Sutskever, and Mark Chen. Glide: Towards photorealistic image generation and editing with text-guided diffusion models. *arXiv preprint arXiv:2112.10741*, 2021. [5](#)
- [20] Aditya Ramesh, Prafulla Dhariwal, Alex Nichol, Casey Chu, and Mark Chen. Hierarchical text-conditional image generation with clip latents. *arXiv preprint arXiv:2204.06125*, 1(2):3, 2022. [2](#), [3](#)
- [21] Yurui Ren, Xiaoming Yu, Junming Chen, Thomas H Li, and Ge Li. Deep image spatial transformation for person image generation. In *Proceedings of the IEEE/CVF Conference on Computer Vision and Pattern Recognition*, pages 7690–7699, 2020. [2](#)
- [22] Robin Rombach, Andreas Blattmann, Dominik Lorenz, Patrick Esser, and Björn Ommer. High-resolution image synthesis with latent diffusion models. In *Proceedings of the IEEE/CVF conference on computer vision and pattern recognition*, pages 10684–10695, 2022. [2](#), [3](#), [4](#), [6](#), [1](#)
- [23] Chitwan Saharia, William Chan, Saurabh Saxena, Lala Li, Jay Whang, Emily L Denton, Kamyar Ghasemipour, Raphael Gontijo Lopes, Burcu Karagol Ayan, Tim Salimans,

- et al. Photorealistic text-to-image diffusion models with deep language understanding. *Advances in Neural Information Processing Systems*, 35:36479–36494, 2022. [2](#), [3](#)
- [24] Christoph Schuhmann, Romain Beaumont, Richard Vencu, Cade Gordon, Ross Wightman, Mehdi Cherti, Theo Coombes, Aarush Katta, Clayton Mullis, Mitchell Wortsman, et al. Laion-5b: An open large-scale dataset for training next generation image-text models. *Advances in Neural Information Processing Systems*, 35:25278–25294, 2022. [2](#), [3](#)
- [25] Uriel Singer, Adam Polyak, Thomas Hayes, Xi Yin, Jie An, Songyang Zhang, Qiyuan Hu, Harry Yang, Oron Ashual, Oran Gafni, et al. Make-a-video: Text-to-video generation without text-video data. *arXiv preprint arXiv:2209.14792*, 2022. [2](#), [3](#)
- [26] Jiaming Song, Chenlin Meng, and Stefano Ermon. Denoising diffusion implicit models. In *International Conference on Learning Representations*, 2021. [4](#), [6](#)
- [27] Khurram Soomro, Amir Roshan Zamir, and Mubarak Shah. Ucf101: A dataset of 101 human actions classes from videos in the wild. *arXiv preprint arXiv:1212.0402*, 2012. [2](#)
- [28] Guy Tevet, Sigal Raab, Brian Gordon, Yoni Shafir, Daniel Cohen-or, and Amit Haim Bermano. Human motion diffusion model. In *The Eleventh International Conference on Learning Representations*, 2023. [2](#), [3](#), [4](#), [6](#)
- [29] Jay Zhangjie Wu, Yixiao Ge, Xintao Wang, Stan Weixian Lei, Yuchao Gu, Yufei Shi, Wynne Hsu, Ying Shan, Xiaohu Qie, and Mike Zheng Shou. Tune-a-video: One-shot tuning of image diffusion models for text-to-video generation. In *Proceedings of the IEEE/CVF International Conference on Computer Vision*, pages 7623–7633, 2023. [2](#), [3](#), [4](#)
- [30] Lijun Yu, Yong Cheng, Kihyuk Sohn, José Lezama, Han Zhang, Huiwen Chang, Alexander G Hauptmann, Ming-Hsuan Yang, Yuan Hao, Irfan Essa, et al. Magvit: Masked generative video transformer. In *Proceedings of the IEEE/CVF Conference on Computer Vision and Pattern Recognition*, pages 10459–10469, 2023. [2](#)
- [31] Lvmin Zhang, Anyi Rao, and Maneesh Agrawala. Adding conditional control to text-to-image diffusion models, 2023. [2](#), [4](#), [6](#)

# Text2AC-Zero: Consistent Synthesis of Animated Characters using 2D Diffusion

## Supplementary Material

- A ballerina performing a dance in a studio.
- An astronaut jumps off a lava floor.
- A mechanical cyborg moves to the right on a sandy beach.
- A robot jumps on a trampoline.
- An astronaut jumps on the moon surface.
- A man lifts dumbbells at the gym.
- A skier running on a snowy road.
- A man shimmy dances in a studio.
- An astronaut with a detailed suit warms up on the moon surface.
- Woody from Toy Story doing jumpy dance.

Figure 1. Prompts used to generate videos for the user study.

### 1. Additional Results

We provide additional **video** results generated by our method and the two approaches in comparison in the [project page](#). Additional image results are also shown in Figures 4 and 5. Note that we use Stable Diffusion [22] version 1.5, and the same seed when generating results for different approaches to produce closely comparable videos.

### 2. User Study

For the user study, we generated 10 videos of various motions and objects using Text2Video-Zero [13], MasaCtrl [5], and our method. The prompts used to generate these videos are provided in Figure 1. We conducted two separate user studies between our method vs. MasaCtrl and ours vs. Text2Video-Zero. Users were asked to select the video where the character has stable/consistent textures throughout the video.

### 3. Cross-Frame Correspondences

We explain why there is a need for computing cross-frame correspondences in Section 3.3 based on DensePose [9]. Figure 2 shows that the DensePose embeddings for two consecutive frames have different distributions for the UV-coordinates. This makes it difficult to track different body parts across frames. By computing cross-frame correspondences based on DensePose, the UV-coordinates are

matched between frames, and we obtain a pixel-wise mapping. This allows propagating various signals between frames, such as the latent codes and RGB values. Note that this mapping is *injective*, meaning that each pixel in frame  $i$  is mapped to a *single* or *no* pixels in frame  $i - 1$ . The unmatched pixels are shown in black in Figure 2 for illustration, but in practice, they are replaced with the original values from the DensePose embedding for frame  $i$ .

### 4. Qualitative Ablation Study

We provide some qualitative examples for the ablation study to complement the quantitative ablation that was provided in the main paper. Figure 3 shows some examples of the contribution of Latent Spatial Alignment (SLA) and Pixel-Wise Guidance (PWG) to achieving temporal consistency. SLA contributes the most and globally harmonizes the video frames. However, it can miss some details, especially at the finer parts of the character, *e.g.* the legs in the first row, and the hands in the second and third row. PWG complements SLA and improves the consistency of the finer parts as it operates on a higher resolution. It is worth mentioning that employing only PWG is not sufficient to achieve reasonable consistency, but only when combined with SLA, can it impact the output. The reason is that SLA aligns the latents making the task of PWG easier in improving the fine details.

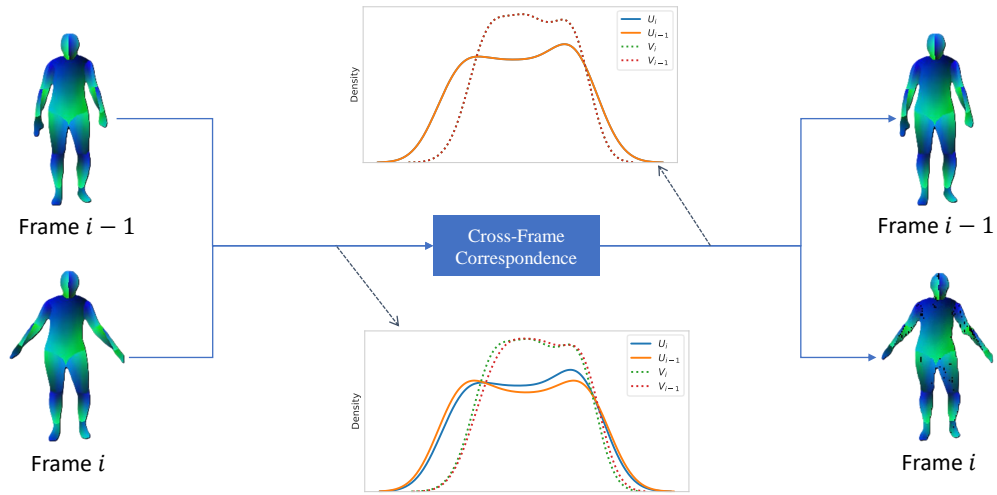


Figure 2. DensePose embeddings for different frames have dissimilar distributions for the UV-coordinates. By computing cross-frame correspondences, we align these coordinates, and we obtain a pixel-wise mapping between the two frames.

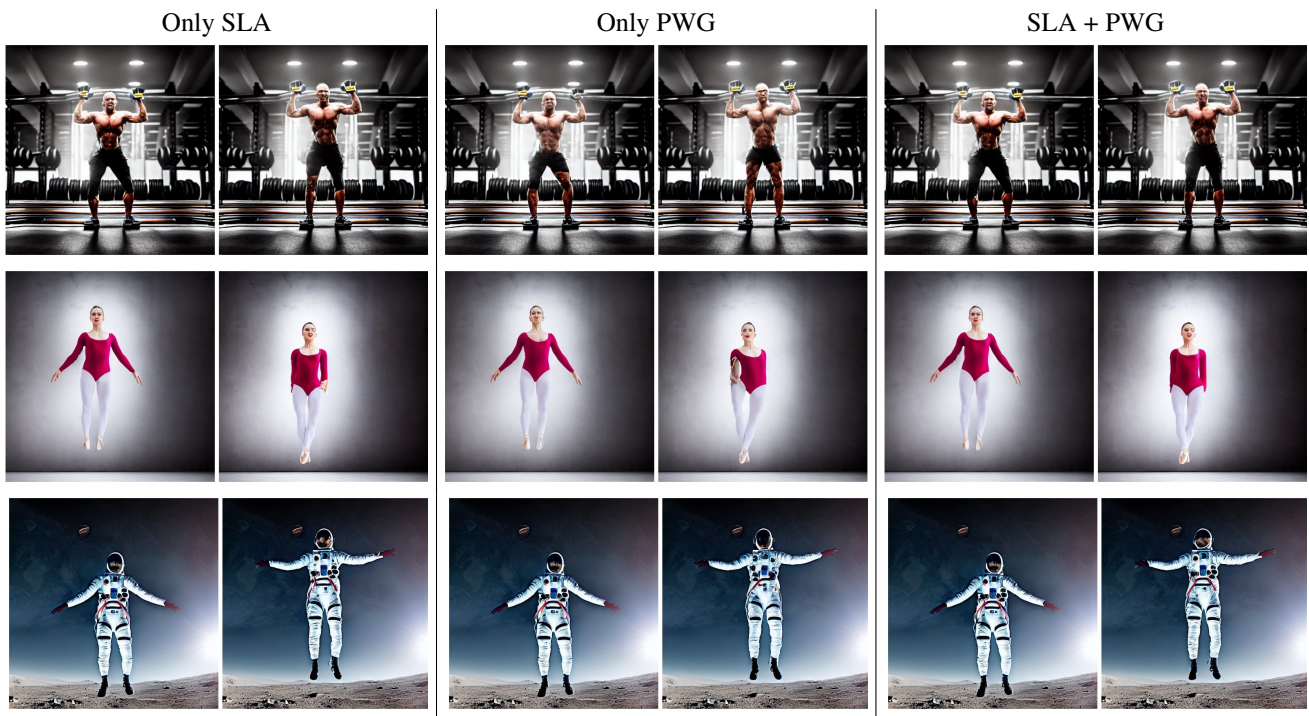
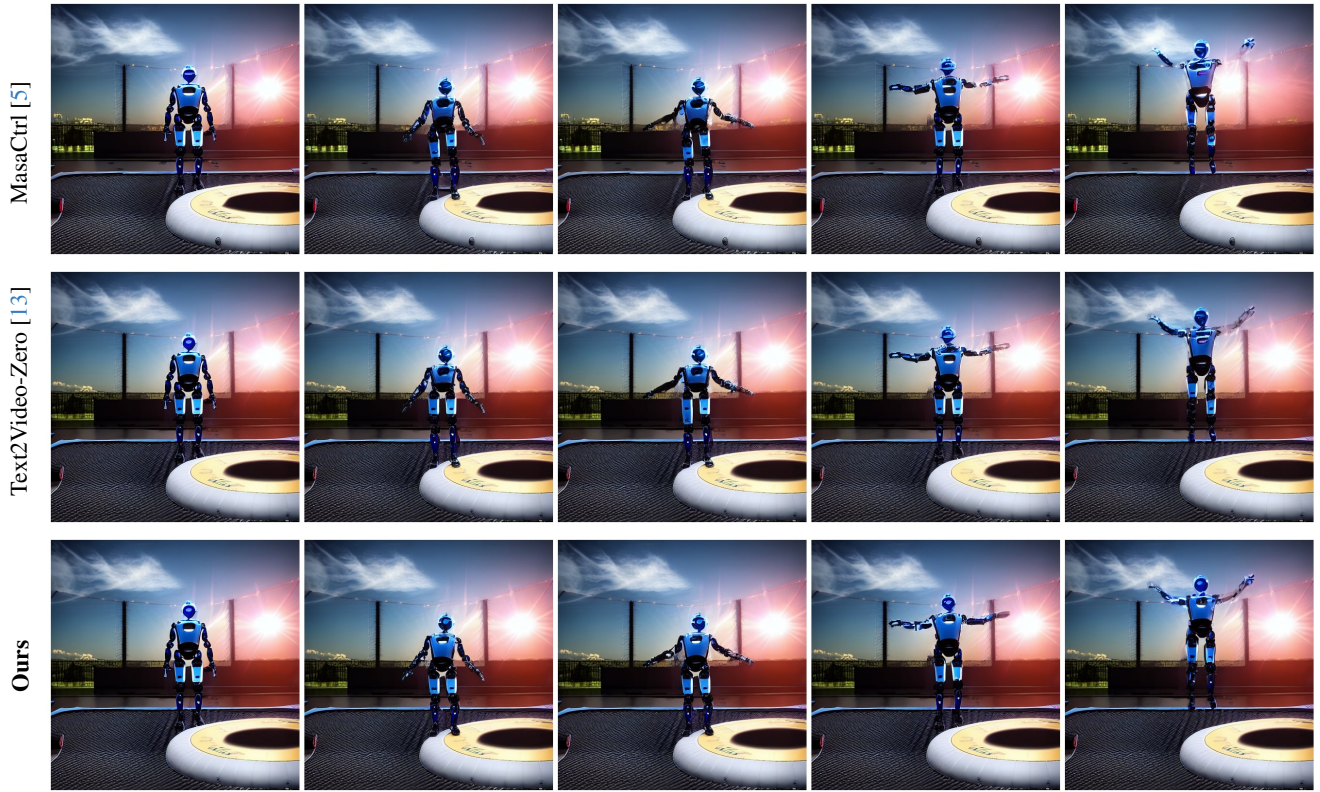


Figure 3. An ablation study for different components of our pipeline: Spatial Latent Alignment (SLA), and Pixel-Wise Guidance (PWG).



Prompt: "A robot jumps on a trampoline"

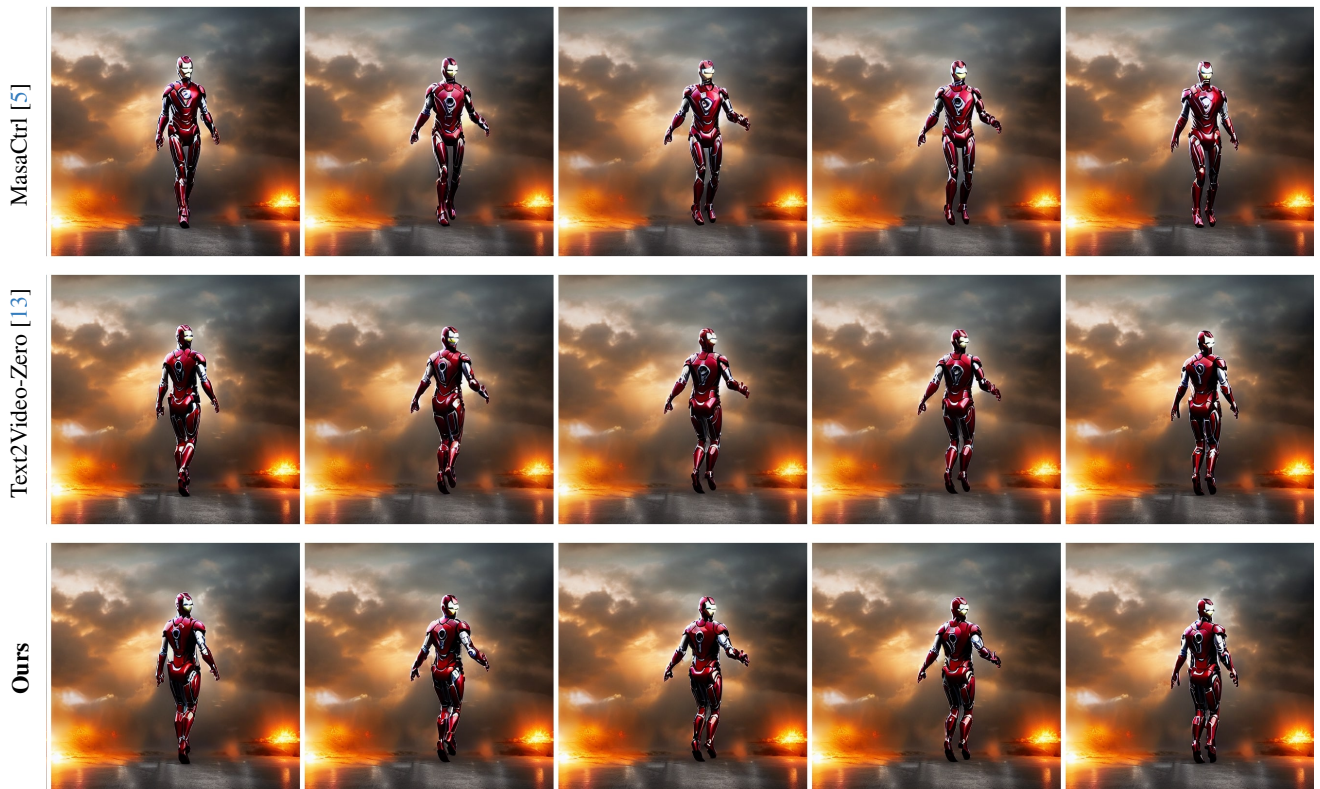


Prompt: "A skier running on a snowy road"

Figure 4. A qualitative comparison between our proposed approach, MasaCtrl [5], and Text2Video-Zero [13].



*Prompt: "An astronaut with detailed suit warms up on the moon surface"*



*Prompt: "Ironman is walking in the street"*

Figure 5. A qualitative comparison between our proposed approach, MasaCtrl [5], and Text2Video-Zero [13].